Critical temperature T_c and Pauli limited critical field of Sr$_2$RuO$_4$: Uniaxial strain dependence

Yue Yu,[1] Stuart Brown,[2] S. Raghu,[1,3] and Kun Yang[4]

[1]*Department of Physics, Stanford University, 476 Lomita Mall, Stanford, California 94305, USA*
[2]*Department of Physics and Astronomy, University of California, Los Angeles, California 90095, USA*
[3]*Stanford Institute for Materials and Energy Sciences, SLAC National Accelerator Laboratory, Menlo Park, California 94025, USA*
[4]*National High Magnetic Field Laboratory and Department of Physics, Florida State University, Tallahassee, Florida 32306, USA*

Variations of critical temperature T_c and in-plane critical field H_{c2} of Sr$_2$RuO$_4$ under uniaxial stress were recently reported. We compare the strain dependence of T_c and H_{c2} in various pairing channels (*d* wave, extended *s* wave, and *p*-wave) with the experimental observations by studying a three-band tight-binding model that includes effects of spin-orbit and Zeeman couplings and a separable pairing interaction. Our study helps narrow down the possibility of pairing channels. The importance of the multiband nature of Sr$_2$RuO$_4$ is also highlighted.

I. INTRODUCTION

Sr$_2$RuO$_4$ has long been one of the best-characterized materials in which unconventional superconductivity condenses out of a Fermi liquid [1,2]. Thus, it presents an almost unique opportunity, where well-controlled theoretical approaches can play a key role in deducing superconducting properties, starting from the underlying electronic structure [3–6]. Nevertheless, several basic phenomenological aspects, including the symmetry of the superconducting order parameter itself, remain unresolved. The results of early NMR spectroscopy measurements [7] and spin-polarized neutron scattering studies [8], together with evidence for time-reversal symmetry breaking (TRSB) [9,10], were all taken to be consistent with a chiral $p_x + ip_y$ state. However, the chiral $p + ip$ state was recently excluded as a possibility due to newly reported measurements of the ^{17}O Knight shifts [11], which revealed a reduced spin susceptibility in the superconducting state. Moreover, the observation was confirmed in independent NMR studies [12], as well as in a spin-polarized neutron scattering study [13].

The measurements reported in Ref. [11] are among several new experimental studies [14–17] in which the application of uniaxial ([100]) stress has placed further constraints on the nature of the Sr$_2$RuO$_4$ order parameter. The induced strain in these experiments acts as a tetragonal symmetry-breaking perturbation. Thus, it is a sensitive probe of multicomponent order parameters that in turn are required for spontaneous TRSB in the superconducting state and can be exploited to reveal more details of its nature. With these recent developments in mind, we are led to reconsider the phenomenological consequences and to see how distinct order parameters behave in the presence of strain.

The particular focus here is on recent experiments [11,15,18] of critical temperature T_c and in-plane critical field H_{c2} in strained crystals. We compute the strain response of T_c and H_{c2} in different pairing channels and compare them with the observations. At the so-called Van Hove strain ($\varepsilon_{aa} = \varepsilon_v$), one of the Fermi sheets, customarily labeled γ in the literature, crosses the Van Hove singularity (VHS) at the boundary of the first Brillouin zone. This Fermi sheet consists of quasiparticles built predominantly from electrons in the d_{xy} orbital, with weak mixing of d_{xz}, d_{yz} orbitals in the presence of atomic spin-orbit coupling. Since the γ sheet has little dispersion in the c direction, the density of states is expected to diverge logarithmically in the neighborhood of the VHS. Therefore, tuning E_F to the VHS results in an expected enhancement of both the transition temperature [15] and the upper critical field [18]. Further, the enhancement of in-plane ($\vec{H}//\mathbf{b}$) critical field was observed to be stronger than that in the critical temperature [15,18]. Here, we compare and contrast the observed behavior to expectations for selected order parameter symmetries.

More specifically, in this work, we analyze the ratio H_{c2}/T_c as a function of uniaxial $\varepsilon_{xx} - \varepsilon_{yy}$ strain by studying BCS theory on a three-band tight-binding model for different pairing channels, including *d*-wave, *p*-wave, and extended-*s*-wave pairing channels, and compare the results with experimental observations. Our study points out a new direction for narrowing down the possible choices of order parameters for Sr$_2$RuO$_4$, and the methods are readily applied to other systems. Besides comparing results obtained for different pairing channels, the importance of the multiband nature of this material is highlighted by comparing results with and without atomic spin-orbit coupling (SOC) and orbital Zeeman effects. Guided by the observation of a field-induced first-order transition from the (low-field) superconducting state [19], we consider the possibility of an inhomogeneous Fulde-Ferrell-Larkin-Ovchinnikov (FFLO) state [2]. Our study of the strain-dependent H_{c2}/T_c in Sr$_2$RuO$_4$ may provide a way to search for the FFLO state elsewhere.

As we explain in more detail below, our key findings are as follows: (1) The strain dependence of the ratio H_{c2}/T_c in the *d*+extended-*s*-wave pairing channel is consistent with the experimental observations, while the *p*-wave pairing channel (analogs of the *B* phase of ^{3}He) is not. (2) The multiband nature of Sr$_2$RuO$_4$, including spin-orbit coupling and the orbital Zeeman effect, is necessary for the correct dependence.

(3) FFLO pairing of quasiparticles on the d_{xy} orbital is not sensitive to the Van Hove strain due to Fermi surface nesting.

This paper is organized as follows. In Sec. II, we introduce the settings in BCS theory and the band structure. In Sec. III, we present the numerical results for different pairing channels with and without multiband effects. In Sec. IV, we extend our study to the FFLO state.

II. THE MODEL

We consider an effective three-band tight-binding-Hamiltonian for t_{2g} (d_{yz}, d_{xz}, d_{xy}) electrons of Sr_2RuO_4 with tetragonal symmetry under the Zeeman effect. The Hamiltonian is given by $H_0 + H_Z + H_{BCS}$, where

$$H_0 = \sum_{\vec{k},a,b,\sigma} h_0^{ab}(\vec{k}) c_{\vec{k}a\sigma}^\dagger c_{\vec{k}b\sigma} + H_{SOC} \qquad (1)$$

and

$$h_0(\vec{k}) = \begin{bmatrix} \epsilon^{yz} & \epsilon^{off} & \\ \epsilon^{off} & \epsilon^{xz} & \\ & & \epsilon^{xy} \end{bmatrix},$$

$$\epsilon^{yz} = -2t_2\tau\cos k_x - 2t_1/\tau\cos k_y - \mu,$$

$$\epsilon^{xz} = -2t_1\tau\cos k_x - 2t_2/\tau\cos k_y - \mu,$$

$$\epsilon^{xy} = -2t_3(\tau\cos k_x + 1/\tau\cos k_y)$$
$$\qquad - 4t_4\cos k_x\cos k_y - 2t_5\cos(2k_x)\cos(2k_y) - \mu,$$

$$\epsilon^{off} = -4t_6\sin k_x\sin k_y. \qquad (2)$$

Here, $c_{\vec{k}a\sigma}^\dagger$ ($c_{\vec{k}a\sigma}$) are creation (annihilation) operators for electrons in $a = d_{yz}, d_{xz},$ or d_{xy} orbitals for spin state $\sigma =\uparrow,\downarrow$, and h_0 is a 3×3 Hamiltonian in orbital space. The parameters were obtained in Ref. [20] by fitting the above tight binding model with experimental data, and the resulting fitting parameters are listed here, $(t_1, t_2, t_3, t_4, t_5, t_6, \mu) = (0.145, 0.016, 0.081, 0.039, 0.005, 0, 0.122)$ eV. Note that the off-diagonal term ϵ^{off} that couples d_{yz} and d_{xz} orbitals is zero from fitting. Here, the three t_{2g} orbitals (d_{yz}, d_{xz}, d_{xy}) transform as a vector under point-group symmetry operations. Hence, the angular momentum operator in this internal coordinate representation is $\mathcal{L}_{bc}^a = -i\epsilon_{abc}$, where ϵ_{abc} is the totally antisymmetric tensor, while spin operators are the standard Pauli matrices. Thus, the spin-orbit coupling is

$$H_{SOC} = \vec{L} \cdot \vec{S} = \lambda \begin{pmatrix} 0 & i\sigma^z & -i\sigma^y \\ -i\sigma^z & 0 & i\sigma^x \\ i\sigma^y & -i\sigma^x & 0 \end{pmatrix}. \qquad (3)$$

The strength of spin-orbit coupling is taken to be $\lambda = 0.032$ eV [20].

We introduce the "hopping ratio" τ to incorporate the effect of uniaxial strain, which modifies the hopping strength along the x and y directions (nearest-neighbor hopping strengths t_1 and t_2) in Eq. (2). Under the above settings, zero uniaxial strain corresponds to hopping ratio $\tau = 1$, while Van Hove strain is around $\tau = 1.055$. Fermi surfaces at zero strain and Van Hove strain are plotted in Fig. 1.
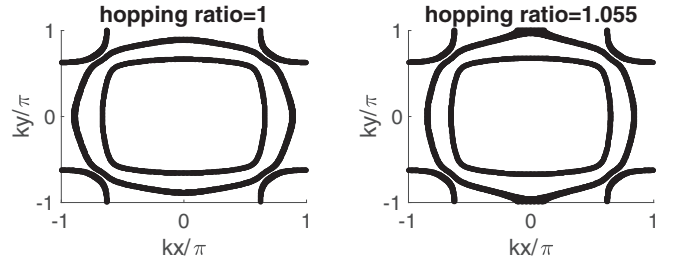

FIG. 1. Fermi surfaces of the three-band tight-binding Hamiltonian in Eq. (2). Left: Zero strain $\tau = 1$, where the system has tetragonal symmetry. Right: Van Hove strain around $\tau = 1.055$, where the γ band touches the boundary of the first Brillouin zone.

The Zeeman field couples to both the spin and orbital, and the resulting Zeeman term is

$$H_Z = -\vec{H} \cdot \vec{\sigma} \otimes \tau_0 + \sigma^0 \otimes \begin{pmatrix} 0 & iH_z & -iH_y \\ -iH_z & 0 & iH_x \\ iH_y & -iH_x & 0 \end{pmatrix}. \qquad (4)$$

Here, we have assumed that the system is strongly type II, so that $\vec{H}$ is the external magnetic field. τ_0 is the identity matrix in orbital space, while σ^0 is the identity matrix in spin space.

In this work, we will consider an approximation that the order parameters are purely on the d_{xy} orbital of Sr_2RuO_4, which are closest to the γ band and most sensitive to the Van Hove strain. It should be noted that order parameters on other bands also contribute to the total gap function. However, they are much less strain sensitive, so variations of T_c and H_{c2} due to pairings on the other bands would otherwise be smooth and analytic. Experimentally, which band contributes most to superconductivity is still being investigated [2]. The general form of the BCS interaction on the d_{xy} orbital can be written as

$$H_{BCS} = -\sum_{\vec{k},\vec{k}',\{\sigma_i\}} V_{\sigma_1\sigma_2\sigma_3\sigma_4}(\vec{k}, \vec{k}') c_{-\vec{k}\sigma_1} c_{\vec{k}\sigma_2} c_{\vec{k}'\sigma_3}^\dagger c_{-\vec{k}'\sigma_4}^\dagger. \qquad (5)$$

Here, σ_i denotes spin up or down. In the following calculations, we assume for simplicity that the above BCS interaction is separable; that is, it is of the following form:

$$V_{\sigma_1\sigma_2\sigma_3\sigma_4}(\vec{k}, \vec{k}') = g f(\vec{k})_{\sigma_2\sigma_1}^\dagger f(\vec{k}')_{\sigma_3\sigma_4},$$
$$\hat{\Delta}_{\sigma_1\sigma_2}(\vec{k}) = \Delta f(\vec{k})_{\sigma_1\sigma_2}. \qquad (6)$$

Then the BCS gap equation can be simplified to

$$\Delta = \sum_{|\epsilon_k|<E_D,\sigma_1\sigma_2} g f(\vec{k})_{\sigma_1\sigma_2} \langle c_{-\vec{k}\sigma_1} c_{\vec{k}\sigma_2} \rangle. \qquad (7)$$

Here $\langle \cdots \rangle$ denotes thermal averaging, and ϵ_k is the normal-state eigenenergy. E_D is an energy cutoff, analogous to the Debye temperature in conventional BCS theory. Given a pairing channel $f(\vec{k})$ and pairing strength g, we can numerically diagonalize the Bogoliubov–de Gennes Hamiltonian and solve for the gap magnitude Δ self-consistently, at arbitrary temperature T, magnetic field H, and hopping ratio τ. The critical temperature can then be determined by the standard procedure. When calculating the response to an in-plane critical field, we neglect the c-axis warping of the Fermi surface and consider a two-dimensional Fermi surface. We

thus neglect the orbital effect of the in-plane magnetic field, and the resulting H_{c2} is the Pauli limited critical field.

In order to better compare the results from different pairing channels, we would like to the fix the gap magnitude at zero temperature, zero magnetic field, and zero uniaxial strain to be the same in all channels, i.e.,

$$\Delta(T = 0, B = 0, \tau = 1) = \Delta_0 \equiv 2.8 \times 10^{-4} \text{ eV.} \quad (8)$$

The magnitude of Δ_0 is chosen such that T_c is O(1) K, which is on the same order as the experimental value [15]. The above fixing is achieved by tuning the BCS interaction strength g in each channel. Those interaction strengths will then be fixed throughout the calculation. That is, we have assumed that the BCS interaction strength g is strain independent. A strain-dependent interaction strength will change the magnitude of T_c and H_{c2}. However, the interaction strength will not affect the ratio T_c/H_{c2}. This is well known in the standard BCS theory without disorder, where T_c and Pauli limited H_{c2} are both proportional to the gap magnitude at zero temperature and zero field, while the proportionality constant depends on only the band structure and type of pairing channel, rather than on the interaction strength [21]. The energy cutoff of the interaction (analogous to Debye temperature for BCS theory) is taken to be $E_D = 10\Delta_0$.

III. RESULTS

In the Sec. III A, we present numerical results for d-wave, p-wave, and $(d + s)$-wave pairing channels, in the absence of spin-orbit coupling and the orbital Zeeman effect. In Sec. III B, we will perform the same calculations, but with SOC and orbital Zeeman effects.

The direct comparison between various order parameters helps narrow down the possible pairing channels in Sr$_2$RuO$_4$. We will also highlight the importance of the multiband nature of Sr$_2$RuO$_4$, as we compare the results between these two sections. It is worth noting that, in the absence of SOC and the orbital Zeeman effect, the problem becomes effectively single orbital.

A. Single band

In this section, we remove the spin-orbit coupling and orbital Zeeman effect in the Hamiltonian. Now the d_{yz} and d_{xz} orbitals will not affect the calculations, and effectively, we end up with the problem on the d_{xy} orbital. It should be noted that the Van Hove strain is shifted to a larger hopping ratio, $\tau = 1.08$.

1. d-wave pairing channel

Let us start with the d-wave pairing channel

$$f(\vec{k})_{\sigma_1\sigma_2} = i\sigma^y_{\sigma_1\sigma_2}(\cos k_x - \cos k_y). \quad (9)$$

T_c and Pauli limited critical field H_{c2} as a function of uniaxial strain (hopping ratio τ) are shown in the left panel of Fig. 2. Both quantities have been normalized to unity at zero strain ($\tau = 1$).

At Van Hove strain $\tau = 1.077$, T_c (blue solid line) is clearly enhanced more significantly than H_{c2} (red dotted line). Therefore, the ratio H_{c2}/T_c decreases when approaching the
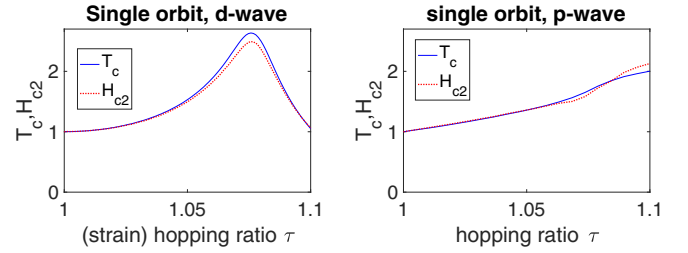

FIG. 2. Critical temperature T_c and Pauli limited critical field H_c for d-wave and p-wave pairing on the single-orbital model as a function of uniaxial strain (hopping ratio τ). Both quantities have been normalized to unity at zero strain ($\tau = 1$). Left: For d-wave pairing, the peak position for the two quantities is at the Van Hove strain. H_{c2} clearly has a weaker enhancement than T_c when approaching the Van Hove strain, which is inconsistent with experimental observation. Right: For p-wave pairing, H_{c2} and T_c are insensitive to the Van Hove singularity at $\tau = 1.077$ since we have assumed that the BCS interaction is strain independent and the p-wave gap function (10) vanishes at $(k_x, k_y) = (0, \pi)$. The ratio H_{c2}/T_c decreases when approaching the Van Hove strain, which is inconsistent with experimental observation.

Van Hove strain, which is inconsistent with the experimental observations.

2. p-wave pairing channel

For spin-triplet superconductors without spin-orbit coupling, Pauli limited critical field cannot be obtained if the $\hat{d}$ vector of the pairing state is perpendicular to the magnetic field. With the presence of SOC (in next section), the above scenario no longer holds, but the resulting H_{c2} could be much bigger than the maximal gap magnitude if SOC is small. Experimentally [18], H_{c2} is found to be of the same order as the maximal gap magnitude $\Delta/g\mu_B$. Noting also that the strain lifts the p_x, p_y degeneracy, states with the d vector parallel to the magnetic field are, in principle, possible. That is, the p-wave pairing channel of the form

$$f(\vec{k})_{\sigma_1\sigma_2} = i(\sigma^x\sigma^y)_{\sigma_1\sigma_2} \sin k_x, \quad (10)$$

arising on the d_{xy} orbital, is considered. The $\hat{d}$ vector is along the x axis, and we calculate the corresponding H_{c2}.

Critical temperature T_c and Pauli limited critical field H_{c2} as a function of uniaxial strain (hopping ratio τ) are shown in the right panel of Fig. 2. Both quantities are normalized to unity at zero strain ($\tau = 1$). T_c (blue solid line) is clearly enhanced more significantly than H_{c2} (red dotted line) at the Van Hove strain $\tau = 1.077$. Therefore, the ratio H_{c2}/T_c decreases when approaching the Van Hove strain, which is inconsistent with the experimental observations.

Under the assumption of a strain-independent BCS interaction strength, the critical temperature and critical field in the p-wave pairing channel are not sensitive to the Van Hove strain, and we do not observe any peak in Fig. 2 at the Van Hove strain. This is because the p-wave gap function $f(\vec{k})$ vanishes at the Van Hove singularity $(k_x, k_y) = (0, \pi)$.
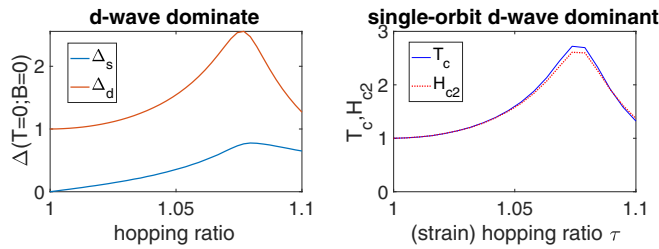
FIG. 3. Results for a mixture of extended-s-wave and d-wave pairing channels in a single-orbital model. A particular set of interaction strengths (g_d, g_s) has been chosen. Left: Pairing magnitude at $T = H = 0$ for each pairing channel as a function of strain. Right: Critical temperature and critical field as a function of strain. The enhancement in H_{c2} is weaker than that in T_c, which is inconsistent with the experimental observation.

3. d +extended-s-wave pairing channel

We now consider the mixture between the d-wave $f(\vec{k})_{\sigma_1\sigma_2} = i\sigma^y_{\sigma_1\sigma_2}(\cos k_x - \cos k_y)$ and extended-s-wave $f(\vec{k})_{\sigma_1\sigma_2} = i\sigma^y_{\sigma_1\sigma_2}(\cos k_x + \cos k_y)$ pairing channels. When applying uniaxial strain, the tetragonal symmetry is broken, and these two pairing channels belong to the same irreducible representation and hence are allowed to mix. In the following calculations, we again consider only pairing on the d_{xy} orbital. We now introduce two BCS interaction strengths, g_d and g_s, for the two channels and assume they are strain independent. We choose strengths g_d and g_s such that the d-wave gap magnitude satisfies Eq. (8), and the gap magnitude of the extended-s-wave pairing channel vanishes at zero strain.

The gap magnitude as a function of uniaxial strain is plotted in the left panel of Fig. 3. Thus, in this calculation, d-wave pairing dominates over the extended-s-wave pairing. We solved the two gap equations and obtained critical temperature and critical field.

At the Van Hove strain $\tau = 1.077$, T_c (blue solid line) is clearly enhanced more significantly than H_{c2} (red dotted line). Therefore, the ratio H_{c2}/T_c decreases on approaching the Van Hove strain, which is inconsistent with the experimental observations.

In this section, we effectively removed d_{yz} and d_{xz} orbitals from the Hamiltonian and obtained H_{c2} and T_c for a single-orbital (d_{xy} orbit) system. We have tried d-wave, p-wave, and d+extended-s-wave pairing channels, but none trend similarly to the experimentally observed ratio H_{c2}/T_c.

B. Three-band system

1. d-wave pairing channel

We start with the d-wave-only pairing channel $f(\vec{k})_{\sigma_1\sigma_2} = i\sigma^y_{\sigma_1\sigma_2}(\cos k_x - \cos k_y)$ for the three-band system. The critical temperature T_c and Pauli limited critical field H_{c2} as a function of uniaxial strain (hopping ratio τ) are shown in the left panel in Fig. 4. Both quantities have been normalized to unity at zero strain (at $\tau = 1$).

H_{c2} (red dotted line) is clearly enhanced more significantly than T_c (blue solid line). Therefore, the ratio H_{c2}/T_c increases when approaching the Van Hove strain, which is consistent with the experimental observations.
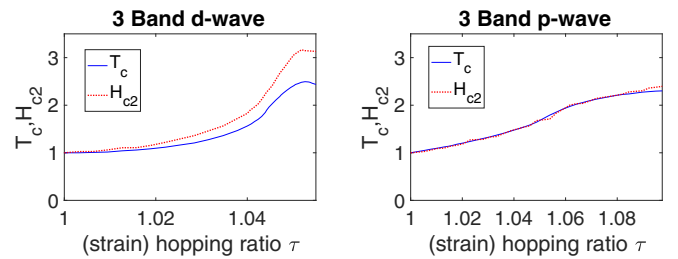
FIG. 4. Critical temperature T_c and Pauli limited critical field H_c for d-wave and p-wave pairing on a three-band model as a function of uniaxial strain (hopping ratio τ). Both quantities have been normalized to unity at zero strain ($\tau = 1$). Left: For d-wave pairing, the peak position for the two quantities is at the Van Hove strain. H_{c2} clearly has a stronger enhancement than T_c when approaching the Van Hove strain, which is consistent with experimental observation. Right: For p-wave pairing, H_{c2} and T_c are not sensitive to the Van Hove singularity since we have assumed that the BCS interaction is strain independent and the p-wave gap function vanishes at the Van Hove singularity $(k_x, k_y) = (0, \pi)$. The ratio H_{c2}/T_c does not change when approaching the Van Hove strain, which is inconsistent with experimental observation.

2. p-wave pairing channel

For reasons mentioned in Sec. III A 2, in order to calculate the Pauli limited critical field, the p-wave pairing state with $f(\vec{k})_{\sigma_1\sigma_2} = i(\sigma^x\sigma^y)_{\sigma_1\sigma_2}\sin k_x$ is considered. The $\hat{d}$ vector is along the x direction, and we calculate critical field also in this direction.

T_c and Pauli limited critical field H_{c2} as a function of uniaxial strain (hopping ratio τ) are shown in the right panel of Fig. 4. Both quantities have been normalized to unity at zero strain (at $\tau = 1$). The enhancements in H_{c2} (red dotted line) and T_c (blue solid line) are almost the same. Therefore, the ratio H_{c2}/T_c does not change when approaching the Van Hove strain, which is inconsistent with the experimental observations.

For the same reasons as in Sec. III A 2, we did not observe any peak in T_c or H_{c2} near the Van Hove strain since the gap function for the p-wave pairing state vanishes at the Van Hove singularity. Again, one could get the correct shape of the peak by introducing strain-dependent BCS interaction strengths, but this will not affect the ratio H_{c2}/T_c.

3. d+extended-s-wave pairing channel

We now turn to a mixture between the d-wave $f(\vec{k})_{\sigma_1\sigma_2} = i\sigma^y_{\sigma_1\sigma_2}(\cos k_x - \cos k_y)$ and extended-s-wave $f(\vec{k})_{\sigma_1\sigma_2} = i\sigma^y_{\sigma_1\sigma_2}(\cos k_x + \cos k_y)$ pairing channels. Similar to the single-orbital case in Sec. III A 3, we choose strengths g_d and g_s, such that the d-wave gap magnitude satisfies Eq. (8), and the gap magnitude of the extended-s-wave pairing channel vanishes at zero strain. Thus, in this calculation, d-wave pairing dominates over the extended-s-wave pairing. The gap magnitude as a function of uniaxial strain is shown in the left panel of Fig. 5. We solved the two gap equations and obtained the critical temperature and critical field.

T_c and H_{c2} as a function of uniaxial strain are summarized in the right panel of Fig. 5. Enhancement of H_{c2} is notably
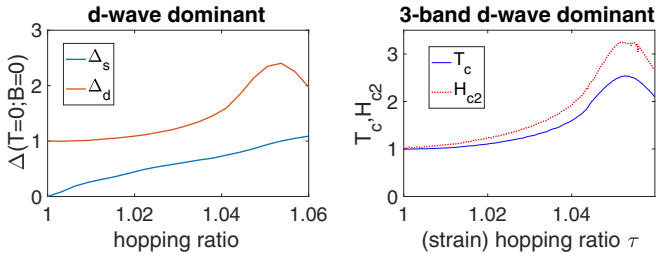
FIG. 5. Results for a mixture of extended-*s*-wave and *d*-wave pairing channels in the three-band model. A particular set of interaction strengths (g_d, g_s) has been chosen. Left: Pairing magnitude at $T = H = 0$ for each pairing channel as a function of strain. Right: Critical temperature and critical field as a function of strain. The enhancement in H_{c2} is stronger than that in T_c, which is consistent with the experimental observation.

stronger than that of T_c. Further, under the strain-independent BCS interaction, enhancement in T_c and H_c at the Van Hove strain agrees quantitatively with experimental observations, with a maximal enhancement around 2.5 to 3 times. The peak position matches the Van Hove strain, at around $\tau = 1.055$.

It is worth noting that g_s/g_d is a free parameter in the calculation. In the calculation of the d+extended-*s*-wave pairing channel, we have chosen $g_d/g_s = 1$, and the calculation of the d-wave-only pairing channel in Sec. III B 1 can be thought of as a special case with $g_s/g_d = 0$. Choices of g_s/g_d do not qualitatively change the results; in the calculation of a stronger extended-*s*-wave pairing channel with $g_s/g_d = 6.7$, where g_s is taken such that the extended-*s*-wave gap magnitude satisfies Eq. (8), the H_{c2}/T_c ratio also increases from zero strain to Van Hove strain by about 30%.

In this section, we have illustrated our numerical results for the ratio H_{c2}/T_c as a function of uniaxial strain for different pairing channels. By comparing the results with experimental observations, we found that the d+extended-*s*-wave pairing channel can provide the correct strain dependence in the ratio H_{c2}/T_c while the p-wave pairing channel cannot.

Comparing the results in these two sections, we summarize that the multiband nature of Sr$_2$RuO$_4$ and d-wave-type pairing channels are the key to explaining the strain dependence of the ratio H_{c2}/T_c.

IV. SINGLE-BAND FFLO STATE

An inhomogeneous FFLO state, with nonzero-momentum Cooper pairs, may appear as an intermediate phase in strong applied fields under the conditions that the Zeeman effect dominates over orbital suppression of the superconducting state [22]. Such conditions otherwise apply in very anisotropic organic superconductors for in-plane fields [23]. And since the applicability of an otherwise isotropic Zeeman effect implies singlet pairing, the evidence for such an intermediate state has been searched for in the case of parallel fields in Sr$_2$RuO$_4$. In only one case that we know of is there a suggestion for a field-induced intermediate phase [24]. Nevertheless, we would like to study the possibility of the d-wave FFLO state on the d_{xy} orbital considered here.

Following [22], we extend the BCS interaction to

$$H_{\text{BCS}} = - \sum_{\vec{k},\vec{k}',\vec{q},\{\sigma_i\}} V_{\sigma_1\sigma_2\sigma_3\sigma_4}(\vec{k},\vec{k}') c_{-\vec{k}\sigma_1} c_{\vec{k}+\vec{q}\sigma_2} c^{\dagger}_{\vec{k}'+\vec{q}\sigma_3} c^{\dagger}_{-\vec{k}'\sigma_4}.$$
(11)

The q dependence in $V(\vec{k},\vec{k}')$ has been neglected. With the assumption of the separable interaction in Eq. (6) and the d-wave pairing channel $f_k = i\sigma_y(\cos k_x - \cos k_y)$, the BCS gap equation can be simplified to

$$1 = \sum_{|\epsilon_k| < E_D} g \frac{(\cos k_x - \cos k_y)^2}{E_k}$$

$$\times \left[\tanh \frac{E_{k+q/2} + H}{2kT} + \tanh \frac{E_{k-q/2} - H}{2kT} \right]. \quad (12)$$

H_{c2} for the FFLO state is the largest field among all possible $\vec{q}$, in which the gap equation has the solution $\Delta = 0$. In this section, we choose interaction strength g such that the zero-momentum state satisfies Eq. (8) with $E_D = 50\Delta_0$.

At zero temperature and zero strain, we found that $H_{c2} \approx 42\Delta_0$ at $\vec{q} \approx 1.8H/v_{F,0}\hat{x}$ (or $\hat{y}$). At Van Hove strain, we found $H_{c2} \approx 39\Delta_0$ at $\vec{q} \approx 2.2H/v_{F,VH}\hat{x}$. Here, $v_{F,0}$ and $v_{F,VH}$ are the Fermi velocities at $k_y = 0$ for zero and Van Hove strain.

The magnitude of the FFLO critical field is found to be much higher than that of the zero-momentum state. This may be due to Fermi surface nesting. The two "vertical" parts in the d_{xy} orbital (see Fig. 1) contribute to nesting and therefore prefer a horizontal pairing momentum $\vec{q}$. This also explains why the FFLO state is not sensitive to the Van Hove singularity, which is not part of the nesting.

Since the critical field of the FFLO state is not sensitive to the Van Hove singularity, the H_{c2}/T_c ratio for FFLO state is therefore inconsistent with experimental observations for Sr$_2$RuO$_4$. However, our study of H_{c2} as a function of uniaxial strain points out a direction to search for FFLO states in other materials.

V. CONCLUSION AND DISCUSSION

We studied the ratio H_{c2}/T_c as a function of uniaxial strain for Sr$_2$RuO$_4$ and tried to match the experimentally observed increased ratio near the Van Hove strain. We considered a three-band tight-binding Hamiltonian with separable and strain-independent BCS interaction on the d_{xy} orbital. We tried different pairing channels and found that the experimental observation can be explained with the d+extended-*s*-wave, rather than the p-wave, pairing state. We removed d_{yz} and d_{xz} orbitals and then found that none of the pairing channels could match the experimental results. Therefore, we concluded that the multiband nature of Sr$_2$RuO$_4$ and d-wave-type pairing channels are the key to explaining the strain dependence of the ratio H_{c2}/T_c.

We also studied the ratio H_{c2}/T_c for the FFLO state. Due to Fermi surface nesting, the d-wave FFLO state on the d_{xy} orbital is not sensitive to the Van Hove strain. However, our study points out a way to test the FFLO state for broader systems.

Last, we discuss our results within the context of the broader phenomenological paradoxes presented by Sr$_2$RuO$_4$.

Prior to the NMR spectroscopy results in Ref. [11], the key phenomenological issues involved rationalizing various experimental observations within the hypothesis of a chiral $p_x + ip_y$ superconducting ground state. The experimental results in Ref. [11] ruled out this scenario. Instead, the focus has shifted towards reconciling the NMR measurements with observations of TRSB in Kerr and muon spectroscopy (μSR) studies.

On the one hand, TRSB requires having two distinct and degenerate order parameters. This can be ensured by symmetry if the order parameter belongs to a multidimensional irreducible representation (irrep). Such states, however, exhibit a split transition in the presence of the uniaxial strain considered in this paper: The absence of such split transitions casts significant doubt on the viability of such explanations. TRSB can also occur in a fine-tuned situation where two distinct irreps become degenerate (see, for instance, the recent proposal in Ref. [25]). Such degeneracy, if present, would be sensitive to perturbations and may well be lifted by strain. Indeed, a recent μSR experiment in the presence of uniaxial strain shows the absence of TRSB at the superconducting transition from the normal state [17]. It is thus reasonable to start with a simpler setting of a single pairing channel when studying the strain effects, which is precisely what we have done here.

[1] A. P. Mackenzie and Y. Maeno, Rev. Mod. Phys. **75**, 657 (2003).

[2] A. P. Mackenzie, T. Scaffidi, C. W. Hicks, and Y. Maeno, npj Quantum Mater. **2**, 40 (2017).

[3] A. Ramires and M. Sigrist, Phys. Rev. B **94**, 104501 (2016).

[4] A. Ramires and M. Sigrist, J. Phys.: Conf. Ser. **807**, 052011 (2017).

[5] A. T. Rømer, A. Kreisel, M. A. Müller, P. Hirschfeld, I. M. Eremin, and B. M. Andersen, arXiv:2003.13340.

[6] H. G. Suh, H. Menke, P. Brydon, C. Timm, A. Ramires, and D. F. Agterberg, arXiv:1912.09525.

[7] K. Ishida, H. Mukuda, Y. Kitaoka, K. Asayama, Z. Q. Mao, Y. Mori, and Y. Maeno, Nature (London) **396**, 658 (1998).

[8] J. A. Duffy, S. M. Hayden, Y. Maeno, Z. Mao, J. Kulda, and G. J. McIntyre, Phys. Rev. Lett. **85**, 5412 (2000).

[9] G. M. Luke, Y. Fudamoto, K. M. Kojima, M. I. Larkin, J. Merrin, B. Nachumi, Y. J. Uemura, Y. Maeno, Z. Q. Mao, Y. Mori *et al.*, Nature (London) **394**, 558 (1998).

[10] J. Xia, Y. Maeno, P. T. Beyersdorf, M. M. Fejer, and A. Kapitulnik, Phys. Rev. Lett. **97**, 167002 (2006).

[11] A. Pustogow, Y. Luo, A. Chronister, Y.-S. Su, D. A. Sokolov, F. Jerzembeck, A. P. Mackenzie, C. W. Hicks, N. Kikugawa, S. Raghu *et al.*, Nature (London) **574**, 72 (2019).

[12] K. Ishida, M. Manago, K. Kinjo, and Y. Maeno, J. Phys. Soc. Jpn. **89**, 034712 (2020).

[13] A. N. Petsch, M. Zhu, M. Enderle, Z. Q. Mao, Y. Maeno, and S. M. Hayden, arXiv:2002.02856.

[14] C. W. Hicks, D. O. Brodsky, E. A. Yelland, A. S. Gibbs, J. A. N. Bruin, M. E. Barber, S. D. Edkins, K. Nishimura, S. Yonezawa, Y. Maeno *et al.*, Science **344**, 283 (2014).

[15] A. Steppke, L. Zhao, M. E. Barber, T. Scaffidi, F. Jerzembeck, H. Rosner, A. S. Gibbs, Y. Maeno, S. H. Simon, A. P. Mackenzie *et al.*, Science **355** eaaf9398 (2017).

[16] Y. S. Li, N. Kikugawa, D. A. Sokolov, F. Jerzembeck, A. S. Gibbs, Y. Maeno, C. W. Hicks, M. Nicklas, and A. P. Mackenzie, arXiv:1906.07597.

[17] V. Grinenko, S. Ghosh, R. Sarkar, J.-C. Orain, A. Nikitin, M. Elender, D. Das, Z. Guguchia, F. Brückner, M. E. Barber *et al.*, arXiv:2001.08152.

[18] Y. Luo, A. Pustogow, P. Guzman, A. P. Dioguardi, S. M. Thomas, F. Ronning, N. Kikugawa, D. A. Sokolov, F. Jerzembeck, A. P. Mackenzie *et al.*, Phys. Rev. X **9**, 021044 (2019).

[19] S. Yonezawa, T. Kajikawa, and Y. Maeno, J. Phys. Soc. Jpn. **83**, 083706 (2014).

[20] V. Zabolotnyy, D. Evtushinsky, A. Kordyuk, T. Kim, E. Carleschi, B. Doyle, R. Fittipaldi, M. Cuoco, A. Vecchione, and S. Borisenko, J. Electron Spectrosc. Relat. Phenom. **191**, 48 (2013).

[21] B. Chandrasekhar, Appl. Phys. Lett. **1**, 7 (1962).

[22] K. Yang and S. L. Sondhi, Phys. Rev. B **57**, 8566 (1998).

[23] J. A. Wright, E. Green, P. Kuhns, A. Reyes, J. Brooks, J. Schlueter, R. Kato, H. Yamamoto, M. Kobayashi, and S. E. Brown, Phys. Rev. Lett. **107**, 087002 (2011).

[24] N. Kikugawa, T. Terashima, S. Uji, K. Sugii, Y. Maeno, D. Graf, R. Baumbach, and J. Brooks, Phys. Rev. B **93**, 184513 (2016).

[25] S. A. Kivelson, A. C. Yuan, B. J. Ramshaw, and R. Thomale, npj Quantum Mater. **5**, 43 (2020).